Ministry of Higher Education

and Scientific Research

Journal of Kufa for Chemical Sciences

A refereed

Research Journal Chemical Sciences

Vol.2 No.8 Year 2022

ISSN 2077-2351

Synthesis, Spectral and Thermal Studies of New Azo Dyes Complexes Derived From 3-tert-butyl-4-hydroxyanisol

Hanadi M. Jarallah, Mouayed Y. Kadhum, Adnan S. Abdulnabi

University of Basrah, College of Education for Pure Science, Department of Chemistry, Basrah, Iraq.

الخلاصة

تم تحضير أصباغ الازو الجديدة المشتقة من ازدواج املاح الدايزونيوم للامينات المعوضة بارا تولودين و 3-أمينوفينول مع (3-tert-butyl-4-hydroxyanisol). كما حضرت مجموعة من المعقدات من تفاعل ليكاندات الازو مع املاح النحاس الثنائي والنيكل الثنائي، شخصت المركبات المحضرة باستخدام مطيافية الاشعة تحت الحمراء ، الرنين النووي المغناطيسي للبروتون والكاربون ، مطيافية الكتلة ، مطيافية الاشعة الفوق بنفسجية ، التوصيلية المولارية ، تحليل العناصر الدقيق ، الحساسية المغناطيسية والتحليل الوزني الحراري. كشفت الدراسات الطيفية والبيانات التحليلية أن ليكاندات اصباغ الازو تعمل كليكاندات ثنائية السن ترتبط مع الايون الفلزي عن طريق O^- من مجموعة الهيدروكسيل و N من مجموعة الازو. القيم الواطئة من قياس التوصيلية المولارية بينت ان جميع المعقدات المحضرة ذات طبيعة غير الكتروليتية، كما تبين أن نسبة التفاعل لتكوين المعقدات بنسبة مولية (2:1) من الايون الفلزي الى الليكاند ولها خواص بارا مغناطيسية. اعتمادًا على النتائج تبين ان معقدات النحاس الثنائي ذات شكل رباعي السطوح بينما معقدات النيكل الثنائي ذات شكل ثماني السطوح. كما بينت التحاليل الحرارية تفكك المعقدات بخطوتين الى ثلاث خطوات، الخطوة الاولى للفقدان تشير الى فقدان الماء المرتبط بالبلورة ، تليها فقدان جزيئات الماء المرتبطة تناسقيا مع الذرة المركزية وبعدها مرحلة تفكك الليكاند.

Abstract

New azo dyes ligand of substituted amines para-toluidin and 3-aminophenol with 3-tert-butyl-4-hydroxyanisol and their complexes with Ni(II) and Cu(II) were synthesized and characterized using (^{1}HNMR, ^{13}CNMR, mass spectrometry, FT-IR, Uv–Vis, molar conductance, elemental analysis, magnetic moment and thermogravimetric analysis). The spectral studies and analytical data revealed that the azo dyes ligands act as bidentate ligands via deprotonated OH and nitrogen atom of the azo group. The low molar conductance data detected that all the metal complexes were non-electrolytic in nature, as well as showed that the reaction ratio was 1:2 metal:ligand and had paramagnetic properties for all metal complexes and had an octahedral geometrical shape for Ni complexes and tetrahedral for Cu complexes. Thermal analysis studies showed the decomposition of the complexes in two to three steps with the weight loss of hydrated water in the first decomposition step followed by the coordinated water and ligand molecules.

Keywords: 3-tert-butyl-4-hydroxyanisol, azo dyes, metal complex, thermal analysis

Introduction

Azo dyes are a type of organic compounds that contains at least one conjugated azo (-N=N-) group as a chromophore. To enhance the color, this chromophoric moiety may be linked to two or more aromatic or heterocyclic rings. Azo dyes can contain more than one azo group and are thus classified as monoazo, diazo, triazo, and so on based on the number of azo moieties in the molecule [1]. Azo compounds are nitrogen compounds that do not occur naturally and are constantly being studied in scientific research [2–4]. Azo dyes are the most broadly used class of coloring materials due to their numerous applications in science and technology [5–7]. They are also produced through the diazotization of aromatic amines and the use of a coupling reagent that contains one or more azo groups (–N=N–) attached to one or more aromatic moieties [8]. Because of their affinity for wool and silk, azo dyes are used in the coloring of fibers[9], photoelectronics[10], optical storage technology [11], biologicalreactions[12], as well as in analytical, and food chemistry[13]. Azo compounds are well known for their medicinal importance and are widely used as antineoplastics[14], antidiabetics[15], antibacterial [16,17], and antitumor agents[18]. They are known to be involved in a variety of biological reactions, including DNA, RNA, and protein synthesis inhibition, carcinogenesis, and nitrogen fixation [19,20], Transition metal complexes of azo compounds are gaining popularity due to their superior dyeing properties in textiles and fibers when compared with free dyes. Fabrics dyed with metal complex dyes have excellent light fastness [21]. Transition metal complexes with azo ligands also have interesting physical, chemical, photophysical, photochemical, catalytic, and material properties [22-24]. Azo complexes have been extensively researched for their medical and biological applications [25]. The present study reports preparation of new azo dyes ligands and their complexes and their identification by spectroscopic and analytical methods and knowledge of their geometric shapes.

2. Experimental

2.1: Materials: Para-toluidin and 3-aminophenol from Merck and used without purification, 3-tert-butyl-4-hydroxy anisol from Fluka, Nickel Chloride hexahydrate and Copper Chloride dihydrate from (B.D.H). TLC plate 20 × 20 cm type silica gel 60 GF 254 (Aluminium) from Merck, Hydrochloric acid (37%) were obtained from Scharlau, triethylamine from Merck, Deionized water was used for the preparation of all solutions.

2.2: Measurements: Melting points were determined on a thermo fisher. FTIR spectra were measured using KBr discs on a Shimadzu-84005. (Uv-Vis) spectra were measured for ($1x10^{-3}$ M) in ethanol using (Uv-Vis 1800 Shimadzu), El-mass spectra of the ligands were recorded on Agilient. ^{1}HNMR and ^{13}CNMR were recorded on a Bruker (400 MHz for ^{1}HNMR and 100 MHz for ^{13}C NMR) using DMSO-d6 as a solvent. Thermal analyses measurements (TGA and DTG) were recorded on a Rheometric Scientific lnc.1998, nitrogen flow rate 10 cm3/min and heating rate 10 c/min. Elemental analysis (CHN) was performed in a CHNS – 932 LECO apparatus.

2.3 : Experimental part

2.3.1 : Preparation of azo ligands (L1 and L2)

The azo dye ligands L1 and L2 (Scheme 1) were prepared in the same way by dissolving 5 mmol, (0.535 and 0.545g) of para-toluidin and 3-aminophenol respectively in 10 mL of distilled water containing (2 mL) of conc. HCl this mixture was stirred until a clear solution was obtained. The mixture was cooled to 0–5 ºC and a cold solution of sodium nitrite (0.38 g) in water (5 mL) was then added dropwise during 5 minute and the reaction mixture was further stirred for 20 min in an ice bath at 0–5 ºC to form the diazonium salt. This solution was then added to a solution containing 5mmol (0.901g) of 3-tert-butyl-4-hydroxyanisol dissolved in 80 mL of ethanol which contained 1.5g of NaOH with keeping temperature at 0–5 ºC. The resulting violet solution was stirred for 60 minute. The mixture was kept in refrigerator for over night and acidified with dilute HCl to pH=6[26]. The product was collected by filtration and washed with distilled water and dried at room temperature overnight, and finally recrystallized twice from ethanol. The purenss of the azo dye ligand was chacked by TLC.

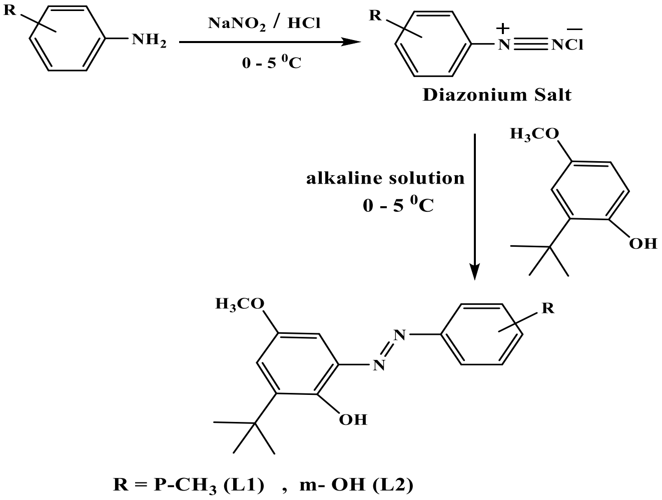

Scheme 1: Synthesis of ligand L1 and L2

2.3.2 : Synthesis of metal Complexes

Metal complexes were prepared by a solution of metal chloride containing (0.237g) and (0.17g), 1mmole of $NiCl_2.6H_2O$ and $CuCl_2.2H_2O$ respectively in 15mL ethanol. These solution were added to a solution of the ligand L1 and L2 (0.596g and 0.6, 2mmole) respectively in ethanol (25mL), in the presence of 1mL triethylamine as basic medium [27]. The reaction mixture was then refluxed for 4-6 hours. The obtained solution was left for 1 h in the freezer[28]. The formed precipitates were filtered off, washed with ethanol, then with diethyl ether and dried in air. The physical properties and C.H.N analysis were shown in Table 1.

Table 1: Physical properties and chemical analysis of azo dyes and their Complexes

Comp.	Empirical formula M.wt.	Colour	m.p °C	Yield %	Λ_M ($Ohm^{-1}.cm^2. mol^{-1}$)	μ_{eff} (B.M)	Elemental analysis % Calculated (found)		
							C	H	N
L1	$C_{18}H_{22}N_2O_2$ 298	Red	120-122	88	---	---	---	---	---
L1Ni	$C_{36}H_{50}N_4O_8Ni$ 724	reddish brown	218-220	66	9.9	2.91	59.66 (58.42)	6.90 (6.15)	7.73 (7.17)
L1Cu	$C_{36}H_{42}N_4O_4Cu$ 657	brown	229-230	76	4.3	1.68	65.75 (63.21)	6.39 (6.01)	8.52 (7.92)
L2	$C_{17}H_{20}N_2O_3$ 300	Dark orange	153-155	84	---	---	---	---	---
L2Ni	$C_{34}H_{48}N_4O_{11}Ni$ 746	brown	> 300	72	8.9	2.87	54.69 (53.43)	6.43 (5.87)	7.50 (7.08)
L2Cu	$C_{34}H_{40}N_4O_7Cu$ 679	Dark brown	> 300	71	13.8	1.66	60.08 (58.92)	5.89 (5.71)	8.24 (7.84)

3. Results and discussion

3.1: FT-IR Spectra

The main vibrational bands of the FTIR spectrum are assigned to the functional groups of the ligands L1 and L2. The spectrum of the L1 (Fig. 1) shows strong bands at 1446 -1467 and 3446 cm^{-1} that are assigned to the ν(N=N) and ν(OH) phenolic respectively. The spectrum of the L2 (Fig. 2) shows strong bands at (1444-1469) and (3466) cm^{-1} that are assigned to the ν(N=N) and ν(OH) phenolic respectively. On complex formation, the bands of ν(N=N) are shifted to lower frequencies by these shifts confirm the coordination of the L1 and L2 through the oxygen of the phenol group and nitrogen of azo group with the metal ions. The spectra of all metal complexes excepted L1Cu complex showed medium and weak broad bands around (3417-3456) cm^{-1} suggesting the existence of water molecules out of coordination sepher (Fig. 3 and 4). The spectra of the complexes exhibit weak bands between (459-493) cm^{-1} and (520-594) cm^{-1} which are attributed to ν(M-N) and ν(M-O) respectively.

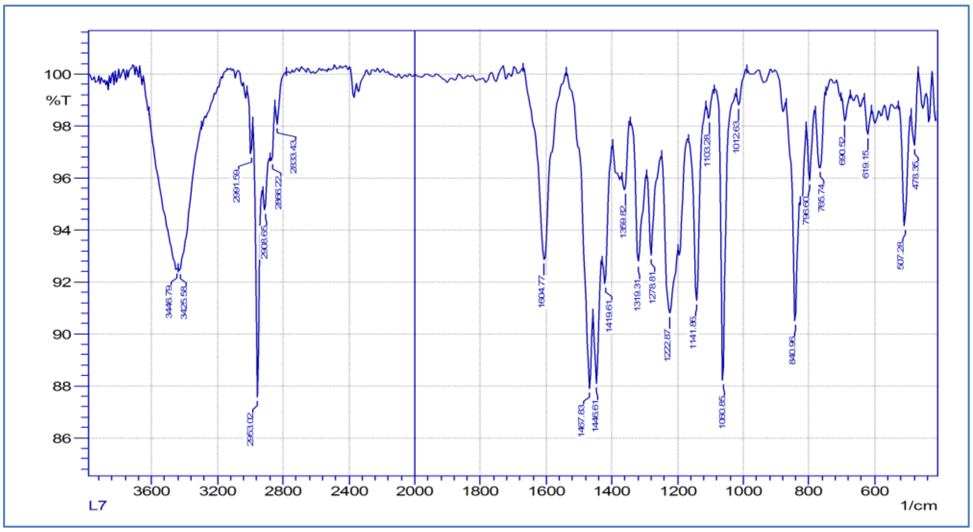

Figure 1: FT-IR Spectrum of the L1

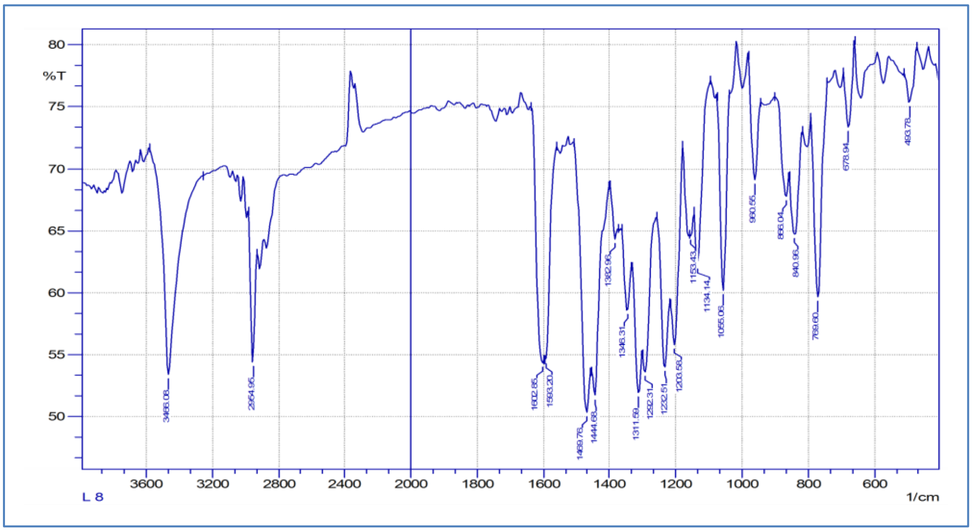

Figure 2: FT-IR Spectrum of the L2

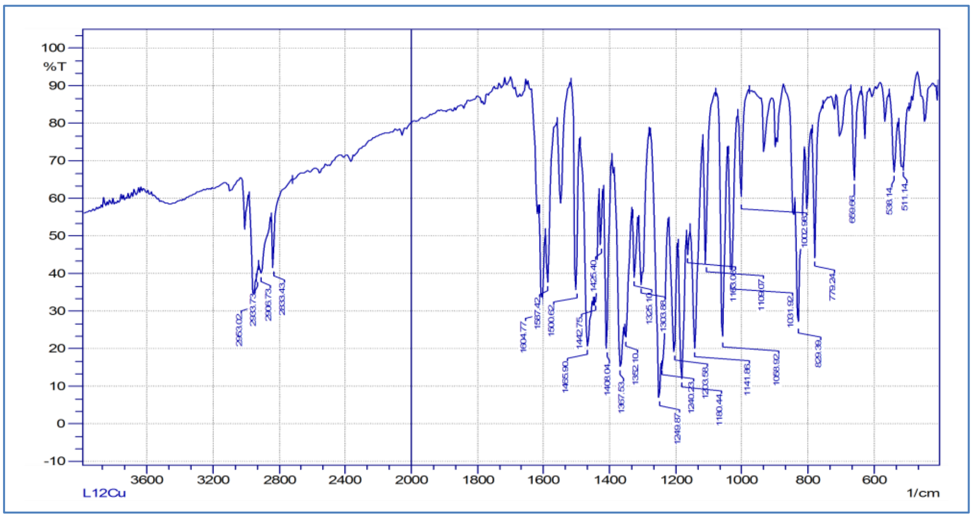

Figure 3: FT-IR Spectrum of L1Cu

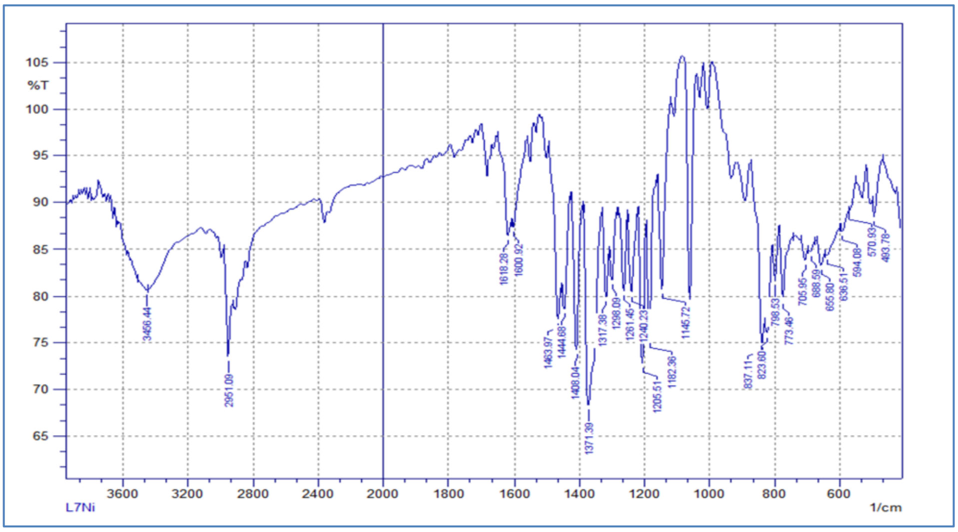

Figure 4: FT-IR Spectrum of L1Ni

3.2: ^{1}HNMR Spectra of ligands

The ^{1}HNMR spectrum was recorded in DMSO-d6 solution using TMS as internal standard. The signal observed at δ 2.49 ppm lead to DMSO-d6. The ^{1}HNMR spectrum of the ligand L1(Fig. 5) show four singlet signals, one of them at δ 11.45ppm (1H) attributed to the phenolic OH group and the other signal at δ 3.76 and 2.39 ppm due to OCH_3 and CH_3 group respectively and a signal at δ 1.41 ppm(9H) due to t-But group, the multiple signal in the range δ 6.95 – 7.96 ppm(6H) attributed to aromatic protons. The ^{1}HNMR spectrum of the ligand L2 (Fig. 6) show also four singlet signal, one of them at δ 3.77 ppm (1H) attributed to OCH_3 group and the other signal at δ 11.8 and 9.8 ppm due to phenolic OH and OH amine group respectively and a signal at δ 1.41 ppm(9H) due to t-But group, the multiple signal in the range δ 6.93– 7.48 ppm(6H) attributed to aromatic protons.

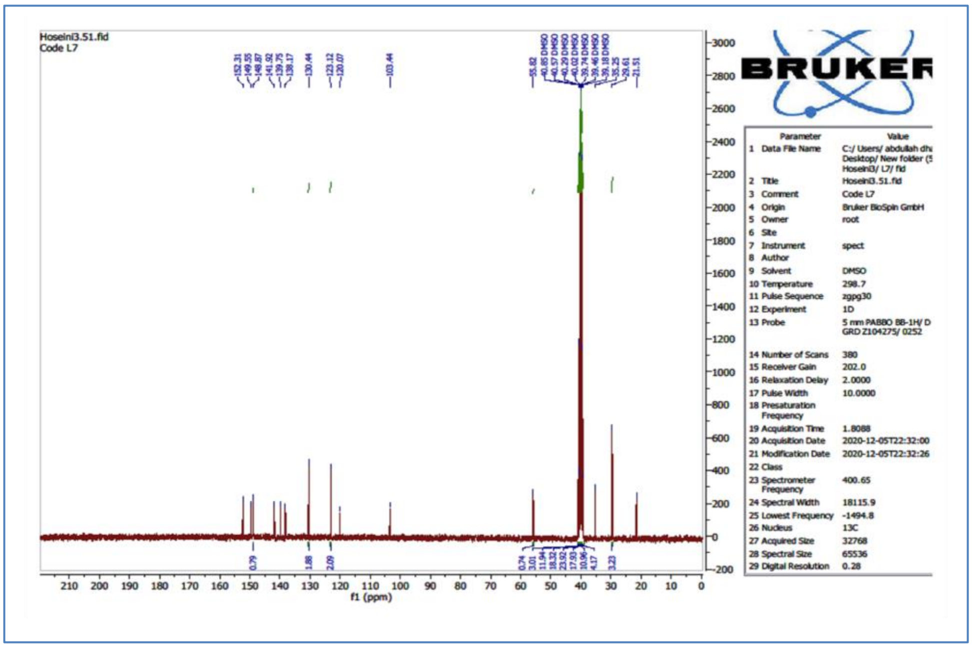

	Parameter	Value
1	Data File Name	C:/ Users/ abdullah dh Desktop/ New folder (Hoseini3/ L7/ fid
2	Title	Hoseini3.51.fid
3	Comment	Code L7
4	Origin	Bruker BioSpin GmbH
5	Owner	root
6	Site	
7	Instrument	spect
8	Author	
9	Solvent	DMSO
10	Temperature	298.7
11	Pulse Sequence	zgpg30
12	Experiment	1D
13	Probe	5 mm PABBO BB-1H/ D GRD Z104275/ 0252
14	Number of Scans	380
15	Receiver Gain	202.0
16	Relaxation Delay	2.0000
17	Pulse Width	10.0000
18	Presaturation Frequency	
19	Acquisition Time	1.8088
20	Acquisition Date	2020-12-05T22:32:00
21	Modification Date	2020-12-05T22:32:26
22	Class	
23	Spectrometer Frequency	400.65
24	Spectral Width	18115.9
25	Lowest Frequency	-1494.8
26	Nucleus	13C
27	Acquired Size	32768
28	Spectral Size	65536
29	Digital Resolution	0.28

Figure 5: ^{1}H NMR Spectrum of L1

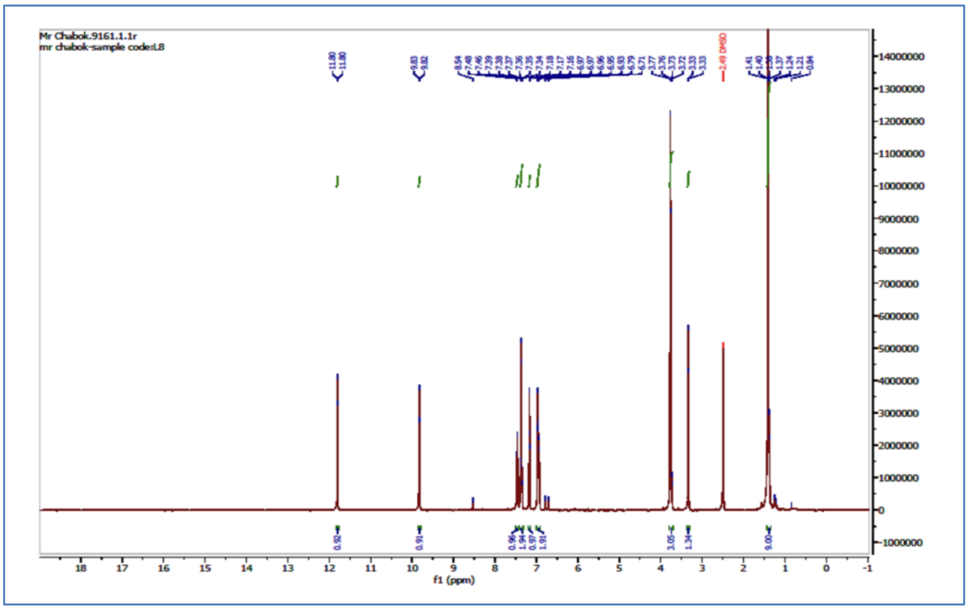

Figure 6: ^{1}H NMR Spectrum of L2

3.3: ^{13}CNMR Spectra

^{13}CNMR spectrum of the L1 ligand (Fig. 7). appears various signals at δ 103.44-152.31 ppm lead to carbon atoms of aromatic rings. The peak at δ 55.82 is assigned to the carbon of OCH_3 group and δ 21.51 ppm due to carbon of CH_3 group, peak at δ 29.61 and 35.25 due to carbon of t-But group.

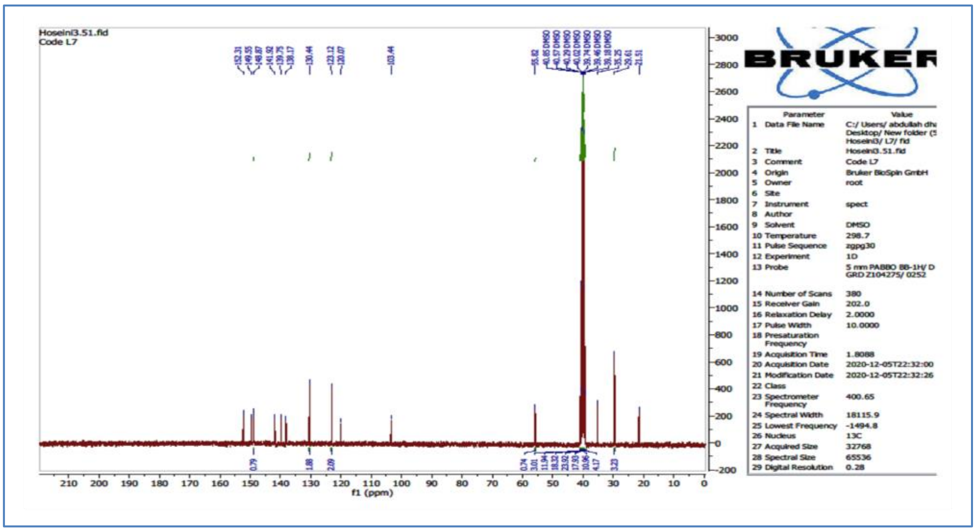

Parameter	Value
1 Data File Name	C:/ Users/ abdullah dh Desktop/ New folder (5 Hosein3/ L7/ fid
2 Title	Hosein3.51.fid
3 Comment	Code L7
4 Origin	Bruker BioSpin GmbH
5 Owner	root
6 Site	
7 Instrument	spect
8 Author	
9 Solvent	DMSO
10 Temperature	298.7
11 Pulse Sequence	zgpg30
12 Experiment	1D
13 Probe	5 mm PABBO BB-1H/ D GRD Z104275/ 0252
14 Number of Scans	380
15 Receiver Gain	202.0
16 Relaxation Delay	2.0000
17 Pulse Width	10.0000
18 Presaturation Frequency	
19 Acquisition Time	1.8088
20 Acquisition Date	2020-12-05T22:32:00
21 Modification Date	2020-12-05T22:32:26
22 Class	
23 Spectrometer Frequency	400.65
24 Spectral Width	18115.9
25 Lowest Frequency	-1494.8
26 Nucleus	13C
27 Acquired Size	32768
28 Spectral Size	65536
29 Digital Resolution	0.28

Figure 7: ^{13}C NMR Spectrum of L1

3.4: Mass Spectra of ligands

The mass spectrum of the ligand L1(Fig. 8) shows the molecular ion at m/z 298.3 This peak undergoes fragmentation to produce peak at m/z 283.3 by losing of methyl molecular. The peaks at m/z 192, 179, 137, 119 and 107 are indicated the breakage of parts of the ligand. The peak at m/z 91.2 with relative abundance 100% (base peak) corresponds to the ion $[C_7H_7]^+$. The mass spectrum of the ligand L2 (Fig. 9) shows the molecular ion at m/z 300.1 with relative abundance

100% (base peak). This peak undergoes fragmentation to produce peak at 285.1 by losing of methel molecular. The peak at m/z 192.1 corresponds to the ion $[C_{11}H_{14}O_2N]^+$.

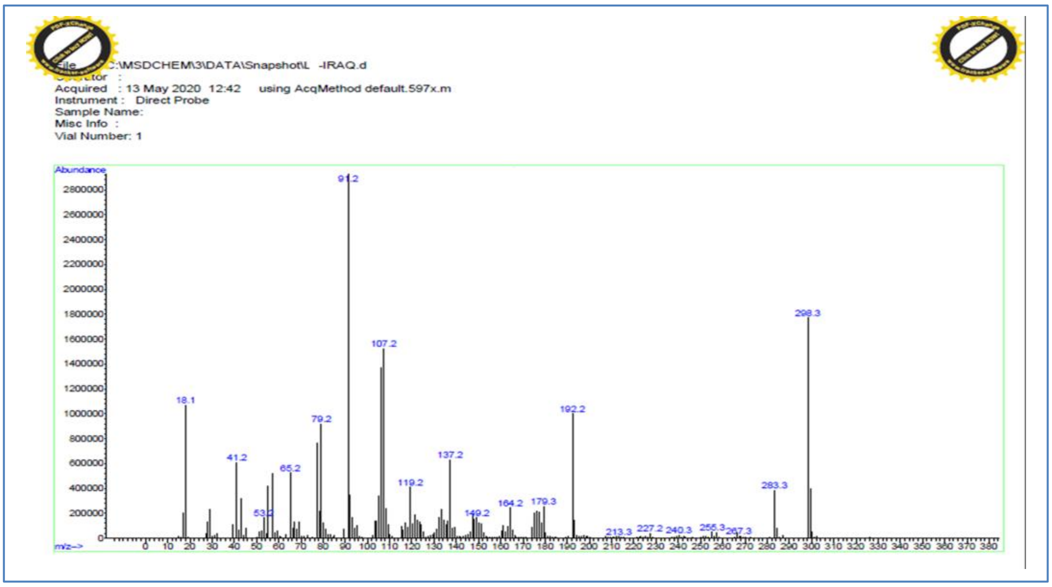

Figure 8: Mass Spectrum of L1

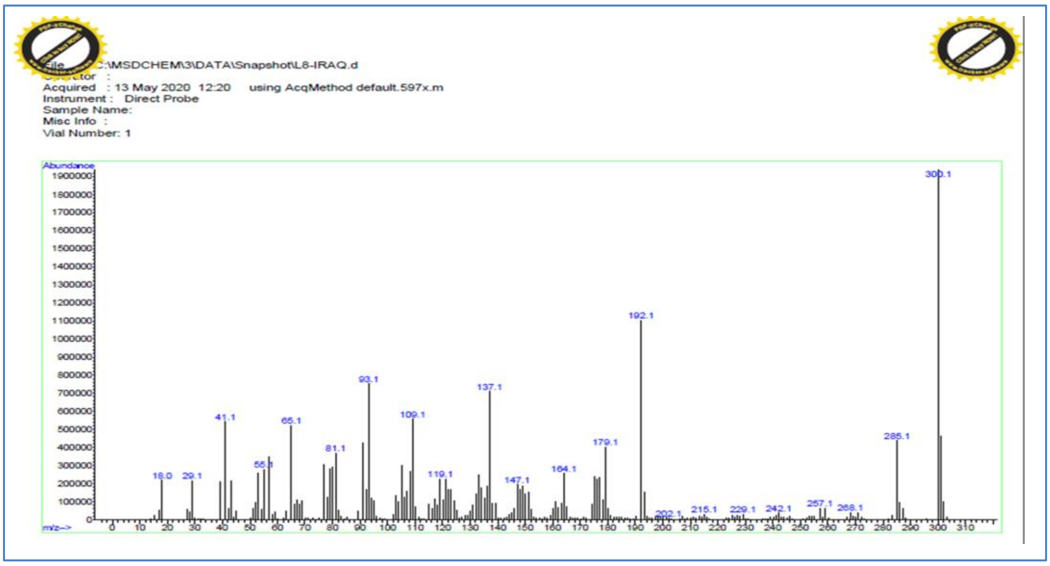

Figure 9: Mass Spectrum of L2

3.5 : Uv–Vis spectra

The Uv–visible spectra of the ligands (L1,L2) and their complexes were recorded in ethanol solution ($1x10^{-3}$ M) at room temperature. The electronic spectra of L1 and L2 (Fig. 10 and 11) respectively showed Uv absorption peaks at 254–257 and 328–337 nm which may be allocated to $\pi\rightarrow\pi^*$ transition of aromatic ring [29]. The visible band (439 and 440 nm) can be attributed to $\pi \rightarrow \pi^*$ transition involving the entire electronic system of the azo-dyes [30]. After coordination, $\pi\rightarrow\pi^*$ transitions were observed at slightly higher wavelength in the complexes. The new bands observed in Cu (II) complexes (Fig. 12) at 523–544 nm attribute to ligand to metal charge transfer [31]. These spectral features support the tetrahedral geometry around Cu (II) center [32]. The spectra of Ni complexes (Fig. 13) were exhibited three absorption peaks at 246-253, 327-330, 429-439 nm which were described to ligand field and charge transfer. Peaks at 580, 629 and 635 nm were assigned to electronic transition type $^3A_2g_{(F)} \rightarrow {}^3T_1g_{(P)}$, $^3A_2g_{(F)} \rightarrow {}^3T_1g_{(F)}$ and $^3A_2g_{(F)} \rightarrow {}^3T_2g_{(F)}$ [33] .

3.6: Magnetic susceptibility

The magnetic susceptibility data of metal complexes were recorded at room temperature. Because of the presence of two unpaired electrons in the L1Ni and L2Ni complexes the magnetic moment value is 2.91 and 2.87 B.M respectively (Paramagnetic), implying high spin and regular octahedral geometry ($t_{2g}^6\ eg^2$) with Sp^3d^2 hybridization[34]. The magnetic moment of the L1Cu and L2Cu complexes is 1.68 and 1.66 B.M respectively due to the presence of one unpaired electron in the d-orbital, which could be a tetrahedral structure with sp^3 hybridization.

3.7: Elemental Analysis and Molar Conductivity of Complexes

Table 1 contains the results of elemental analysis of the synthesized metal complexes, along with their physical properties. The metal complexes are partially soluble in most organic solvents but completely soluble in dimethylformamide and dimethylsulphoxide. The results of the complexes elemental analyses indicate that metal ions react with the azo dye ligand in a 1:2 ratio, (metal:ligand). Based on these results, the corresponding probable formulae of the metal complexes were suggested as given in the same table. The low molar conductance values measured in DMF (10^{-3} M) solution fall in the ($\Lambda_M = 4.3–13.8\ \Omega^{-1}\ cm^2\ mol^{-1}$) range, indicating the non electrolytic nature of these complexes.

3.8: Thermogravimetric Analysis

Thermogravimetric analysis (TG) of coordination compounds provides very idealistic information on their structures, thermal properties, intermediate nature, and final products of thermal decomposition stages. The TGA and DTG curves of Ni(II) and Cu (II) complexes were recorded at an ambient temperature up to 700°C under N_2 gas flow and a heating rate suitably controlled at 10 °C/min. The stages of decomposition, temperature range, DTG peak temperature, decomposition product loss as well as found and the calculated mass loss percentages were shown in table 2.

The TG curve of L1Cu complex (Fig. 14) showed stability up to 225 °C, there is no crystalline water or coordinated water in this complex because up to a temperature of 225 °C there is no weight loss [35,36]. Therefore the first step began at 225°C which represent the decomposition of ligand parts. The L2Cu complex undergoes decomposition in two steps, the first step in the rang 30-180 °C which represent a loss one lattice water molecule, (theoretical 2.65%, found 2.38%) . The second step at 200-420 °C with present loss 48.96 (theoretical 49.01%) which may be attributed to loss $C_{22}H_{28}O_2$. The L1Ni (Fig. 15) and L2Ni complex undergoes decomposition in three steps, loss rates are shown in the table 2, first step refers to loss crystalline water molecule, the second step correspond to the loss two coordinated water molecule. The third step represents the decomposition of ligand parts[32].

Table 2: Thermal decomposition data of the Complexes

complex	stage	TG range °C	DTG$_{max}$ °C	Mass loss %		Assignment
				Found	Calcu.	
L1Cu	I	225-310	250	49.11	49.31	$C_{22}H_{28}O_2$
L2Cu	II	30-180	50	2.38	2.65	H_2O
	II	200-420	375	48.96	49.01	$C_{22}H_{28}O_2$
L1Ni	I	30-120	80	4.76	4.97	$2H_2O$
	II	125-230	200	5.05	5.23	$2H_2O$
	III	240-330	275	22.01	22.08	$C_{10}H_{24}$
L2Ni	I	30-120	70	7.05	7.23	$3H_2O$
	II	150-290	220	5.11	5.20	$2H_2O$
	III	300-460	365	28.07	28.35	$C_{12}H_{10}O_2$

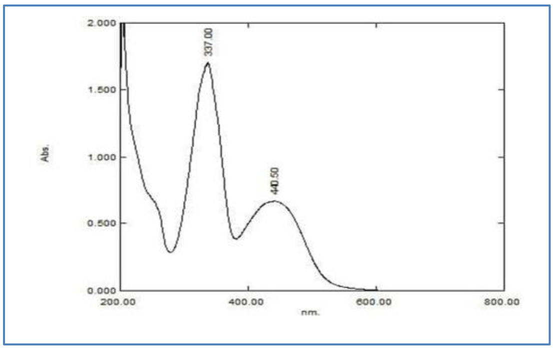

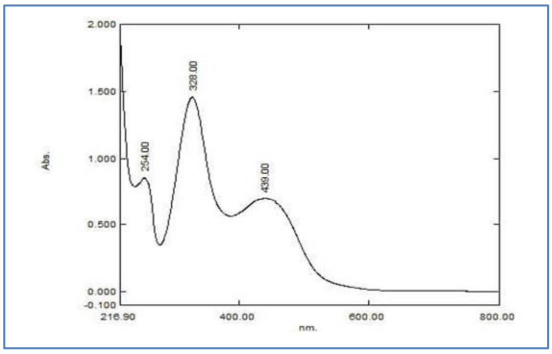

Figure 10: Uv-V is spectrum of the L1 **Figure 11: Uv-V is spectrum of the L2**

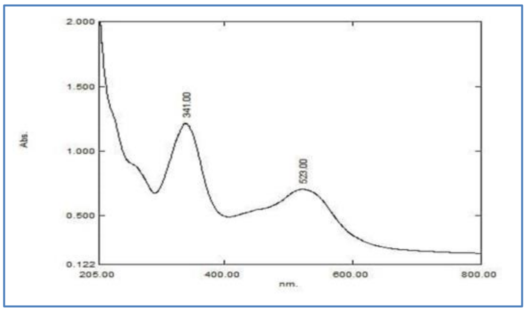

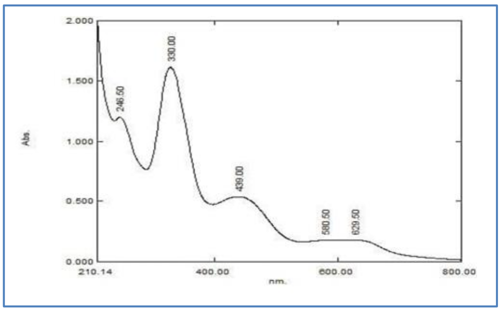

Figure 12: Uv-Vis spectrum of the L1Ni complex

Figure 13: Uv-Vis spectrum of the L1Cu complex

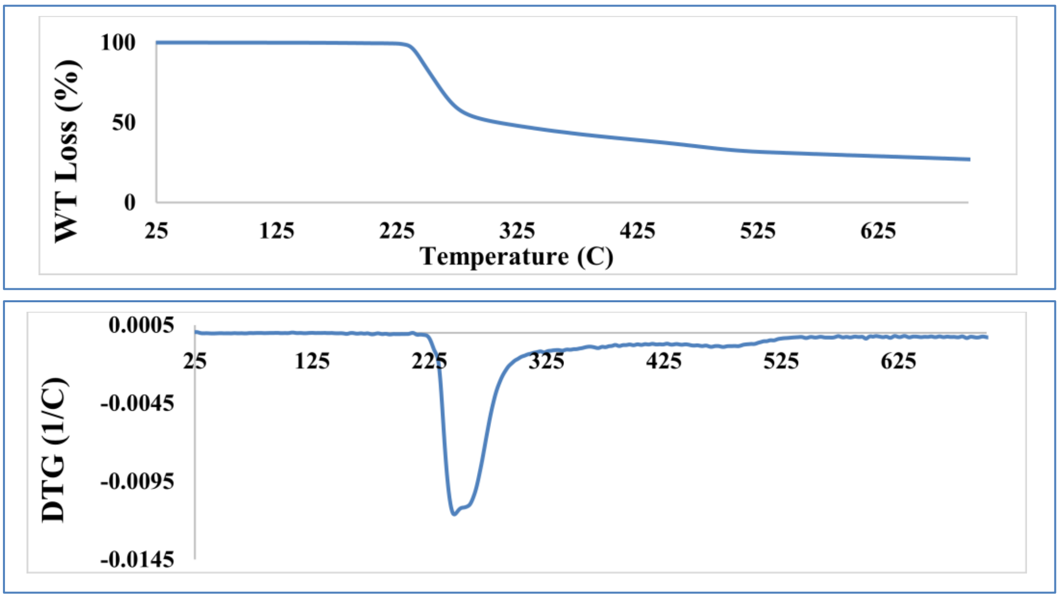

Figure 14: TG and DTG Curve of complex L1Cu

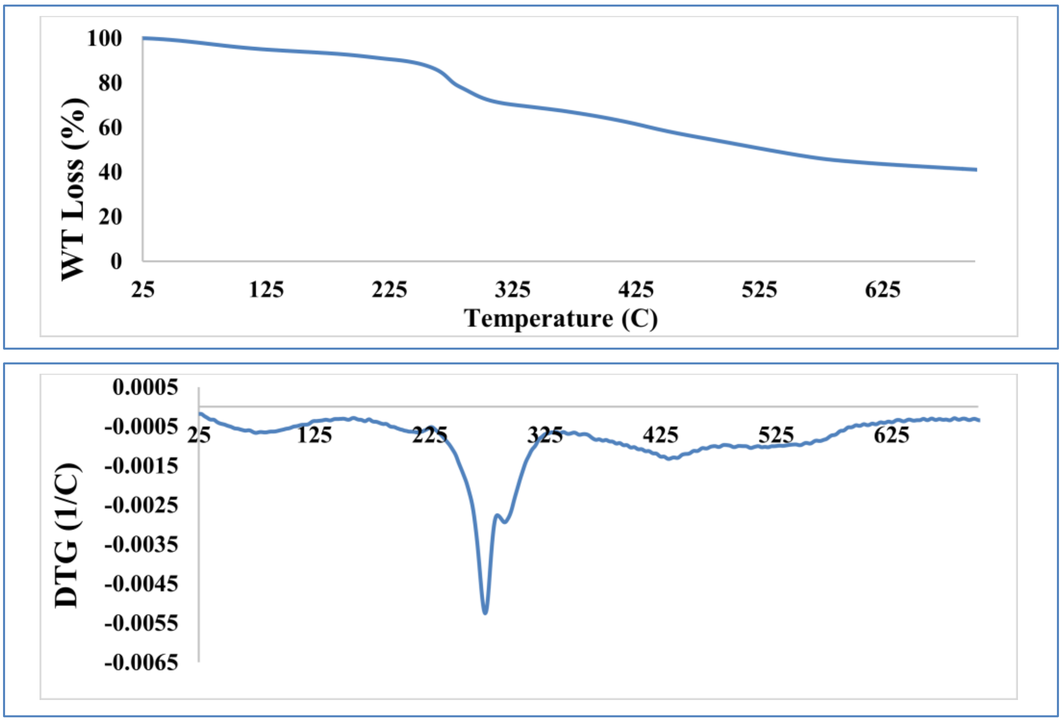

Figure 15: TG and DTG Curve of complex L1Ni

Conclusions

The azo ligands and their metal complexes with Ni(II) and Cu(II) were characterized by FT-IR, Uv–Vis, ^{1}HNMR and ^{13}CNMR spectroscopy, as well as elemental analysis and thermogravimetric analysis. Because of the presence of unpaired electrons, the magnetic moments of synthesized complexes are 2.91, 2.87 and 1.68, 1.66 B.M for Ni(II) and Cu(II) complexes, respectively. For all complexes, the molar conductivity value is consistent with that of non-electrolytes. The synthesized complexes are coordinated by N of azo group and the deprotenated phenolic oxygen. The octahedral geometry has been suggested to Ni(II) complexes, while tetrahedral of Cu(II) complexes.The thermal stability of complexes were studied by TG-DTG diagrams and it was found that the complexes had good thermal stability, and some complexes do not contain crystalline water.

Based on the diagnostic methods and the results of analytical and spectroscopic measurements the metal complexes can be formulated as presented in (Fig. 16).

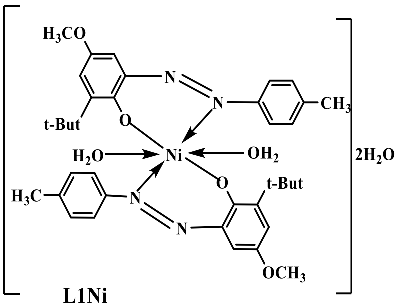

L1Ni

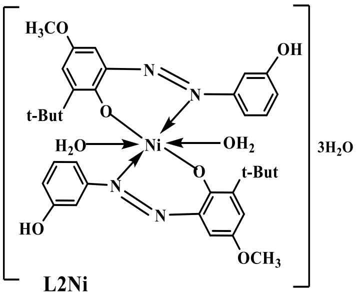

L2Ni

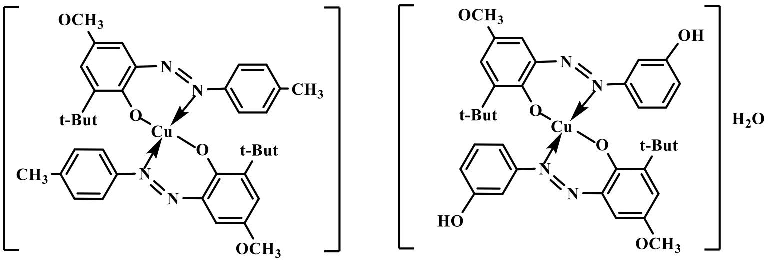

L1Cu L2Cu

Figure 16:Chemical Structure of complexes

References

[1] Santra P. K., Das D., Misra T. K., Roy R., Sinha C., and Peng S.-M., [1999]: Chemistry of azopyrimidines: Synthesis, spectral characterization, electrochemistry and X-ray crystal structure of bis [2-(arylazo) pyrimidine] complexes of copper (I), *Polyhedron*, 18 (14), p 1909–1915.

[2] Kirkan B. and Gup R.,[2008]: Synthesis of new azo dyes and copper (II) complexes derived from barbituric acid and 4-aminobenzoylhydrazone, *Turkish J. Chem.*, 32 (1), p 9–17.

[3] Otutu J. O. and others, [2013]: Synthesis and application of azo dyes derived from 2-Amino-1, 3, 4-thiadiazole-2-thiol on polyester fibre., *Int. J. Res. Rev. Appl. Sci.*, 15 (2), p 292–296.

[4] Seferouglu Z.,[2009]: A study on tautomeric equilibria of new hetarylazo-6-aminouracils., *Ark. Online J. Org. Chem.*, 7, p 42-57.

[5] Dakiky M. and Nemcova I.,[2000]: Aggregation of o, o?-Dihydroxy azo Dyes III. Effect of cationic, anionic and non-ionic surfactants on the electronic spectra of 2-hydroxy-5-nitrophenylazo-4-[3-methyl-1-(4 ?-sulfophenyl)-5-pyrazolone], *Dye. Pigment.*, 44 (3), p 181–193.

[6] Navarro A. and Sanz F., [1999]: Dye aggregation in solution: study of CI direct red I, *Dye. Pigment.*, 40 (2–3), p 131–139.

[7] Tao J., Mao G., and Daehne L., [1999]: Asymmetrical molecular aggregation in spherulitic dye films, *J. Am. Chem. Soc.*, 121 (14), p 3475–3485.

[8] Sener I., Karci F., Kilic E., and Deligöz H., [2004]: Azocalixarenes. 3: synthesis and investigation of the absorption spectra of hetarylazo disperse dyes derived from calix [4] arene, *Dye. Pigment.*, 62 (2), p 141–148.

[9] Patel D. R. and Patel K. C., [2011]: Synthesis of some new thermally stable reactive dyes having 4 (3H)-quinazolinone molecule for the dyeing of silk, wool, and cotton fibers, *Fibers Polym.*, 12 (6) p 741.

[10] Sekar N., [1999]: Ecofriendly metal complex dyes-an update, *Colourage*, 46, p 63–65.

[11] Wang S., Shen S., and Xu H., [2000]: Synthesis, spectroscopic and thermal properties of a series of azo metal chelate dyes, *Dye. Pigment.*, 44 (3), p 195–198.

[12] W\keglarz-Tomczak E. and Górecki Ł., [2012]: Barwniki azowe--aktywność biologiczna i strategie syntezy, *Chemik*, 66 (12), p 1298-1307.

[13] Abdalla N. A., El-Haty M. T., Adam F. A. E., and Hassan F. W., [2013]: Complexes of Cu (II), Co (II), Ni (II), Zn (II), Zr (IV), Ce (III), La (III) AND UO2 (II) with arylazo pyriimidine derivatives, *Re vue Roum. Chim.*, 58 (11–12), p 899–913.

[14] Child R. G., Wilkinson R. G., and Tomcu-Fucik A.,[1977]: Effect of substrate orientation of the adhesion of polymer joints, in *Chem. Abstr*, 87, p 6031.

[15] Garg H. G. and Prakash C., [1972]: Potential antidiabetics. 11. Preparation of 4-arylazo-3, 5-disubstituted-(2H)-1, 2, 6-thiadiazine 1, 1-dioxides, *J. Med. Chem.*, 15 (4), p 435–436.

[16] Khalid A., Arshad M., and Crowley D. E., [2008]: Accelerated decolorization of structurally different azo dyes by newly isolated bacterial strains, *Appl. Microbiol. Biotechnol.*, 78 (2), p 361–369.

[17] Pagga U. and Brown D., [1986]: The degradation of dyestuffs: Part II Behaviour of dyestuffs in aerobic biodegradation tests, *Chemosphere*, 15 (4), p 479–491.

[18] Farghaly T. A. and Abdallah Z. A., [2008]: Synthesis, azo-hydrazone tautomerism and antitumor screening of N-(3-ethoxycarbonyl-4, 5, 6, 7-tetrahydro-benzo [b] thien-2-yl)-2-arylhydrazono-3-oxobutanamide derivatives, *Arkivoc*, 17, p 295–305.

[19] Park C. *et al.*, [2007]: Optimization and morphology for decolorization of reactive black 5 by Funalia trogii, *Enzyme Microb. Technol.*, 40 (7), p 1758–1764.

[20] Hussain G. *et al.*, [2017]: Journal of Applied Research and Technology, *J. Appl. Res. Technol.*, 15, p 346–355,.

[21] Perkins W. S., [1996]: Dyes, *Text. Color. Finish. Perkins WS, Ed. Ed.; Carolina Acad. Press Durham, NC*, p 138–144.

[22] Joseph K. L. V. *et al.*, [2016]: Cyanoacetic acid tethered thiophene for well-matched LUMO level in Ru (II)-terpyridine dye sensitized solar cells, *Dye. Pigment.*, 126, p 270–278.

[23] Neuthe K. *et al.*, [2014]: Phosphonic acid anchored ruthenium complexes for ZnO-based dye-sensitized solar cells, *Dye. Pigment.*, 104, p 24–33.

[24] Guo L., Deng J., Zhang L., Xiu Q., Wen G., and Zhong C., [2012]: Synthesis and applications of 3, 6-carbazole-based conjugated side-chain copolymers containing complexes of 1, 10-phenanthroline with Zn (II), Cd (II) and Ni (II) for dye-sensitized solar cells, *Dye. Pigment.*, 92 (3), p 1062–1068.

[25] Dhahir S. A., Aziz N. M., and Bakir S. R., [2012]: Synthesis, characterization and antimicrobial studies of complexes of some metal ions with 2-[2-amino-5-(3, 4, 5-trimethoxy-benzyl)-pyrimidinyl-4-azo]-4-bromo-phenol, *Red*, 180 (182), p. 69.

[26] Salman S. D. and Adnan S., [2018]: Synthesis, characterization of Some New Derivatives of (Oxazpine, Thiazinone and Hydroquinazoline) Azo group from Amine compounds,”

Eurasian Chem. J., 20 (3), p 264–276.

[27] El-Wakiel N. A., [2016]: Synthesis and characterization of azo sulfaguanidine complexes and their application for corrosion inhibition of silicate glass, *Appl. Organomet. Chem.*, 30 (8), p 664–673.

[28] Erdem E., Sari E. Y., Kilinçarslan R., and Kabay N., [2009]: Synthesis and characterization of azo-linked Schiff bases and their nickel (II), copper (II), and zinc (II) complexes, *Transit. Met. Chem.*, 34 (2), p 167–174.

[29] Debnath P. *et al.*, [2019]: Synthesis, structural characterization and antimicrobial activities of triorganotin (IV) azo-carboxylates derived from ortho/para-amino benzoic acids and $β$-naphthol, *Inorganica Chim. Acta*, 498, p 119172.

[30] Jber N. R., [2011]: Synthesis and Spectral Study of New Azo - Azomethine Dyes and its Copper (II) Complexes Derived from Resorcinol, 4-Aminobenzoylhydrazone and 4-Amino antipyrine, *J. Al-Nahrain Univ. Sci.*, 14 (4), p 50–56.

[31] Roy M., Devi S. S., Roy S., Singh C. B., and Singh K. S., [2015]: Synthesis, characterization, crystal structures and in vitro antimicrobial activities of triorganotin (IV) complexes of azo-dicarboxylates, *Inorganica Chim. Acta*, 426, p 89–98.

[32] El-Sonbati A. Z., Diab M. A., El-Bindary A. E. B., Shoair A. F., Hussein M. A., and El-Boz R. A., [2017]: Spectroscopic, thermal, catalytic and biological studies of Cu(II) azo dye complexes, *J. Mol. Struct.*, 1141, p 186–203.

[33] Jarad A. J. and Quiasim S. H., [2018]: Synthesis and characterization of azo dyes ligands complexes with Ni (II) and Cu (II) and studies their industrial and bacterial application; Res, *J. Pharm. Biol. Chem. Sci*, 9 (2), p 631–642.

[34] Al-Adilee K. J. and Hatem B. A., [2015]: Synthesis and Spectral Characterization of New Azo Dye Derived from Benzimidazole and its Complexation with Selected Transition metal ions," *J. Adv. Chem.*, 11 (3), p 3412–3425.

[35] Bushra K. A., Rehab G. A., Hanadi M. J. and Zuhair A. A., [2015]: Synthesis, spectral and thermal properties of complexes derived from 2-(2-hydroxyphenylimino) methyl-6 methoxyphenol, *J. Chem. Pharm. Res.*, 7(2), p 917-923**.**

[36] Hanadi M. J. and Jabbar S. H., [2012]: Synthesis, characterization and thermal studies of 4-(2-hydroxy-3-methoxybenzylidene amino) -N-(pyridine -2-yl) Benzene Sulphonamide and their complexes, *J. Basr. Res. Sci.*, 38 (1).